Publication Year	2015
Acceptance in OA	2020-03-26T11:13:38Z
Title	The most powerful flaring activity from the NLSy1 PMN J0948+0022
Authors	D'Ammando, F., Orienti, M., Finke, J., RAITERI, Claudia Maria, Hovatta, T., Larsson, J., Max-Moerbeck, W., Perkins, J., Readhead, A. C. S., Richards, J. L., Beilicke, M., Benbow, W., Berger, K., Bird, R., Bugaev, V., Cardenzana, J. V., Cerruti, M., Chen, X., Ciupik, L., Dickinson, H. J., Eisch, J. D., Errando, M., Falcone, A., Finley, J. P., Fleischhack, H., Fortin, P., Fortson, L., Furniss, A., Gerard, L., Gillanders, G. H., Griffiths, S. T., Grube, J., Gyuk, G., Håkansson, N., Holder, J., Humensky, T. B., Kar, P., Kertzman, M., Khassen, Y., Kieda, D., Krennrich, F., Kumar, S., Lang, M. J., Maier, G., McCann, A., Meagher, K., Moriarty, P., Mukherjee, R., Nieto, D., de Bhróithe, A. O'Faoláin, Ong, R. A., Otte, A. N., Pohl, M., Popkow, A., Prokoph, H., Pueschel, E., Quinn, J., Ragan, K., Reynolds, P. T., Richards, G. T., Roache, E., Rousselle, J., Santander, M., Sembroski, G. H., Smith, A. W., Staszak, D., Telezhinsky, I., Tucci, J. V., Tyler, J., Varlotta, A., Vassiliev, V. V., Wakely, S. P., Weinstein, A., Welsing, R., Williams, D. A., Zitzer, B.
Publisher's version (DOI)	10.1093/mnras/stu2251
Handle	http://hdl.handle.net/20.500.12386/23590
Journal	MONTHLY NOTICES OF THE ROYAL ASTRONOMICAL SOCIETY
Volume	446

Monthly Notices
of the
ROYAL ASTRONOMICAL SOCIETY

MNRAS **446,** 2456–2467 (2015) doi:10.1093/mnras/stu2251

The most powerful flaring activity from the NLSy1 PMN J0948+0022

F. D'Ammando,[1,2★†] M. Orienti,[2] J. Finke,[3†] C. M. Raiteri,[4] T. Hovatta,[5] J. Larsson,[6†] W. Max-Moerbeck,[7†] J. Perkins,[8†] A. C. S. Readhead,[5†] J. L. Richards,[9†] and the VERITAS Collaboration, M. Beilicke,[10] W. Benbow,[11] K. Berger,[12] R. Bird,[13] V. Bugaev,[10] J. V. Cardenzana,[14] M. Cerruti,[11] X. Chen,[15,16] L. Ciupik,[17] H. J. Dickinson,[14] J. D. Eisch,[14] M. Errando,[18] A. Falcone,[19] J. P. Finley,[9] H. Fleischhack,[16] P. Fortin,[11] L. Fortson,[20] A. Furniss,[21] L. Gerard,[16] G. H. Gillanders,[22] S. T. Griffiths,[23] J. Grube,[17] G. Gyuk,[17] N. Håkansson,[15] J. Holder,[12] T. B. Humensky,[24] P. Kar,[25] M. Kertzman,[26] Y. Khassen,[13] D. Kieda,[25] F. Krennrich,[14] S. Kumar,[12] M. J. Lang,[22] G. Maier,[16] A. McCann,[27] K. Meagher,[28] P. Moriarty,[22] R. Mukherjee,[18] D. Nieto,[24] A. O'Faoláin de Bhróithe,[16] R. A. Ong,[29] A. N. Otte,[28] M. Pohl,[15,16] A. Popkow,[29] H. Prokoph,[16] E. Pueschel,[13] J. Quinn,[13] K. Ragan,[30] P. T. Reynolds,[31] G. T. Richards,[28] E. Roache,[11] J. Rousselle,[29] M. Santander,[18] G. H. Sembroski,[9] A. W. Smith,[25] D. Staszak,[30] I. Telezhinsky,[15,16] J. V. Tucci,[9] J. Tyler,[30] A. Varlotta,[9] V. V. Vassiliev,[29] S. P. Wakely,[32] A. Weinstein,[14] R. Welsing,[16] D. A. Williams[21] and B. Zitzer[33]

Affiliations are listed at the end of the paper

Accepted 2014 October 24. Received 2014 October 23; in original form 2014 August 6

ABSTRACT

We report on multifrequency observations performed during 2012 December–2013 August of the first narrow-line Seyfert 1 galaxy detected in γ-rays, PMN J0948+0022 ($z = 0.5846$). A γ-ray flare was observed by the Large Area Telescope on board *Fermi* during 2012 December–2013 January, reaching a daily peak flux in the 0.1–100 GeV energy range of $(155 \pm 31) \times 10^{-8}$ ph cm^{-2} s^{-1} on 2013 January 1, corresponding to an apparent isotropic luminosity of $\sim$1.5 $\times$ 10^{48} erg s^{-1}. The γ-ray flaring period triggered *Swift* and Very Energetic Radiation Imaging Telescope Array System (VERITAS) observations in addition to radio and optical monitoring by Owens Valley Radio Observatory, Monitoring Of Jets in Active galactic nuclei with VLBA Experiments, and Catalina Real-time Transient Survey. A strong flare was observed in optical, UV, and X-rays on 2012 December 30, quasi-simultaneously to the γ-ray flare, reaching a record flux for this source from optical to γ-rays. VERITAS observations at very high energy ($E > 100$ GeV) during 2013 January 6–17 resulted in an upper limit of $F_{>0.2\,\mathrm{TeV}} < 4.0 \times 10^{-12}$ ph cm^{-2} s^{-1}. We compared the spectral energy distribution (SED) of the flaring state in 2013 January with that of an intermediate state observed in 2011. The two SEDs, modelled as synchrotron emission and an external Compton scattering of seed photons from a dust torus, can be modelled by changing both the electron distribution parameters and the magnetic field.

Key words: galaxies: active – galaxies: individual: PMN J0948+0022 – galaxies: nuclei – galaxies: Seyfert – gamma-rays: general.

1 INTRODUCTION

Relativistic jets are the most powerful manifestations of the release of energy produced by super-massive black holes in the centres

★Fermi LAT Collaboration Member.
†E-mail: dammando@ira.inaf.it

of active galactic nuclei (AGNs). In about 15 per cent of AGN, the accretion disc is at the base of a bipolar outflow of relativistic plasma, which may extend well beyond the host galaxy, forming the spectacular lobes of plasma visible in radio. The jet emission is observed across the entire electromagnetic spectrum. When the jet axis is closely aligned with our line of sight, the rest-frame radiation is strongly amplified due to Doppler boosting with a large fraction of the output observed at high energy, giving rise to the blazar phenomenon. Radio galaxies are typically viewed at larger angles, with a less extreme amplification of the emission (Urry & Padovani 1995). As a consequence, a very small fraction of radio galaxies is observed at high energy (Ackermann et al. 2011). The discovery in 2008 by the Large Area Telescope (LAT) on board the *Fermi* satellite of γ-ray emission from radio-loud narrow-line Seyfert 1s (NLSy1) revealed the presence of a possible new class of AGNs with relativistic jets. PMN J0948+0022 was the first NLSy1 detected by *Fermi*-LAT (Abdo et al. 2009a), followed by the detection of four other NLSy1s in γ-rays (Abdo et al. 2009b; D'Ammando et al. 2012).

NLSy1 is a class of AGN identified by Osterbrock & Pogge (1985) and defined in terms of the optical properties of its members: narrow permitted lines (FWHM (Hβ) $< 2000\,\mathrm{km\,s^{-1}}$), [O III]/H$\beta$ < 3, and a bump due to Fe II (see e.g. Pogge 2000, for a review). Variability and spectral properties from radio to γ-ray bands, together with the spectral energy distribution (SED) modelling, indicate a blazar-like behaviour of these individual objects (e.g. Abdo et al. 2009b; Foschini et al. 2012; D'Ammando et al. 2013b). One of the most surprising aspects related to these NLSy1s was the detection of flaring activity in γ-rays. A few strong γ-ray flares were observed from PMN J0948+0022 (Donato 2010; Foschini 2010; D'Ammando & Ciprini 2011), with an apparent isotropic γ-ray luminosity up to 10^{48} erg s^{-1}, comparable to that of the bright flat spectrum radio quasars (FSRQ; e.g. PKS 1510−089; Orienti et al. 2013). Similar γ-ray flares have been observed from two other NLSy1s: SBS 0846+513 (Donato 2011; D'Ammando et al. 2013b) and 1H 0323+342 (Carpenter & Ohja 2013). In addition, the high apparent γ-ray luminosity observed in these objects suggests a large Doppler boosting and thus a small viewing angle, similar to blazars. These are important indications that NLSy1s are able to host relativistic jets as powerful as those in blazars.

PMN J0948+0022 could be considered the archetypal object of a new class of γ-ray emitting AGNs; therefore, several multifrequency campaigns were performed to investigate in detail its characteristics over the whole electromagnetic spectrum (Abdo et al. 2009c; Foschini et al. 2011, 2012; D'Ammando et al. 2014). New γ-ray flaring activity from PMN J0948+0022 was detected by *Fermi*-LAT in 2013 January (D'Ammando & Orienti 2013), triggering follow-up observations in optical, UV, and X-rays by *Swift*, and for the first time at very high energy (VHE; $E > 100$ GeV) by the Very Energetic Radiation Imaging Telescope Array System (VERITAS). These data are complemented by the monitoring campaigns performed by the Owens Valley Radio Observatory (OVRO) and the Monitoring Of Jets in Active galactic nuclei with VLBA Experiments (MOJAVE[1]) at 15 GHz, and by the Catalina Real-time Transient Survey (CRTS[2]) in the V band.

The aim of the paper is to discuss the radio-to-γ-ray activity from PMN J0948+0022 during 2012 December–2013 August. This allows us to characterize the SED of the 2013 flaring state of the source in order to compare the SED with that from a different activity state observed in 2011 May, to investigate the emission mechanisms of this source and to discuss its properties in the context of the blazar scenario.

The paper is organized as follows. In Sections 2 and 3, we report the LAT and VERITAS data analysis and results, respectively. The X-ray, UV, and optical data collected by *Swift* are presented in Section 4, together with the optical data collected by CRTS. Radio data collected by the OVRO 40 m telescope and MOJAVE are presented in Section 5. In Section 6, we discuss the properties of the source and the modelling of the SEDs, and draw our conclusions in Section 7.

Throughout the paper, the quoted uncertainties are given at the 1σ level, unless otherwise stated, and the photon indices are parametrized as $\mathrm{d}N/\mathrm{d}E \propto E^{-\Gamma_\nu}$, where Γ_ν is the photon index at the different energy bands. We adopt a Λ cold dark matter cosmology with $H_0 = 71\,\mathrm{km\,s^{-1}\,Mpc^{-1}}$, $\Omega_\Lambda = 0.73$, and $\Omega_\mathrm{m} = 0.27$. The corresponding luminosity distance at $z = 0.5846$ (Schneider et al. 2010), the source redshift, is $d_\mathrm{L} = 3413$ Mpc, and 1 arcsec corresponds to a projected size of 6.59 kpc.

2 *FERMI*-LAT DATA: ANALYSIS AND RESULTS

The *Fermi*-LAT is a pair-conversion telescope operating from 20 MeV to > 300 GeV. It has a large peak effective area ($\sim 8000\,\mathrm{cm^2}$ for 1 GeV photons), an energy resolution of typically ∼10 per cent, and a field of view of about 2.4 sr with single-photon angular resolution (68 per cent containment radius) of $0.^\circ6$ at $E = 1$ GeV on-axis. Further details about the *Fermi*-LAT are given in Atwood et al. (2009).

The LAT data reported in this paper were collected from 2012 December 1 (MJD 56262) to 2013 August 31 (MJD 56535). During this time, the *Fermi* observatory operated almost entirely in survey mode. The analysis was performed with the SCIENCETOOLS software package version v9r32p5.[3] Only events belonging to the 'Source' class were used.[4] The time intervals when the rocking angle of the LAT was greater than 52° were rejected. In addition, a cut on the zenith angle (<100°) was applied to reduce contamination from the Earth limb γ-rays, which are produced by cosmic rays interacting with the upper atmosphere. The spectral analysis was performed with the instrument response functions `P7REP_SOURCE_V15` using an unbinned maximum-likelihood method implemented in the tool `gtlike`. Isotropic (iso_source_v05.txt) and Galactic diffuse emission (gll_iem_v05_rev1.fit) components were used to model the background.[5] The normalizations of both components were allowed to vary freely during the spectral fitting.

We analysed a region of interest of 10° radius centred at the location of PMN J0948+0022. We evaluated the significance of the γ-ray signal from the source by means of the maximum-likelihood test statistic $\mathrm{TS} = 2\,(\log L_1 - \log L_0)$, where L is the likelihood of the data given the model with (L_1) or without (L_0) a point source at the position of PMN J0948+0022 (e.g. Mattox et al. 1996). The source model used in `gtlike` includes all of the point sources from the second *Fermi*-LAT catalogue (2FGL; Nolan et al. 2012) and the preliminary list of the third *Fermi*-LAT catalogue (3FGL; Ackermann et al., in preparation) that fall within 15° of the source. The

[1] http://www.physics.purdue.edu/MOJAVE/
[2] http://crts.caltech.edu/
[3] http://fermi.gsfc.nasa.gov/ssc/data/analysis/software/
[4] http://fermi.gsfc.nasa.gov/ssc/data/analysis/documentation/Cicerone/Cicerone_LAT_IRFs/IRF_overview.html
[5] http://fermi.gsfc.nasa.gov/ssc/data/access/lat/BackgroundModels.html

spectra of these sources were parametrized by power-law (PL) functions, except for 2FGL J0909.1+0121 and 2FGL J1023.6+0040 for which we used a log-parabola (LP) as in the 2FGL catalogue. A first maximum-likelihood analysis was performed in the 0.1–100 GeV energy range to find and remove from the model those sources that have TS $<$ 10 and/or the predicted number of counts based on the fitted model $N_{\rm pred} < 3$. A second maximum-likelihood analysis was performed on the updated source model. In the fitting procedure, the normalization factors and the photon indices of the sources lying within 10° of PMN J0948+0022 were left as free parameters. For the sources located between 10° and 15° from our target, we kept the normalization and the photon index fixed to the values from the 2FGL catalogue or from the 3FGL catalogue for those sources not reported in the former catalogue.

Integrating over the period 2012 December 1–2013 August 31 (MJD 56262–56535) in the 0.1–100 GeV energy range, using an LP, $dN/dE \propto (E/E_0)^{-\alpha-\beta\ \log(E/E_0)}$, as in the 2FGL catalogue, the fit yielded for PMN J0948+0022 a TS = 638, with an average flux of $(15.5 \pm 1.1) \times 10^{-8}$ ph cm^{-2} s^{-1}, a spectral slope of $\alpha = 2.55 \pm 0.08$ at the reference energy $E_0 = 271$ MeV, and a curvature parameter $\beta = 0.05 \pm 0.02$. Using a simple PL, we obtained a TS = 630, with a photon index of $\Gamma = 2.62 \pm 0.06$ and an average flux of $(15.9 \pm 1.0) \times 10^{-8}$ ph cm^{-2} s^{-1}. We used a likelihood ratio test (LRT) to check a PL model (null hypothesis) against an LP model (alternative hypothesis). These values may be compared, following Nolan et al. (2012), by defining the curvature test statistic $TS_{\rm curve} = (TS_{\rm LP} - TS_{\rm PL})$. The LRT results in a $TS_{\rm curve} = 8$, corresponding to an $\sim 2.8\sigma$ difference; therefore, a hint of curvature was observed in the γ-ray spectrum of PMN J0948+0022 during 2012 December–2013 August. By considering only the period 2012 December 1–2013 June 14, in which the source was regularly detected on weekly time-scales, the maximum-likelihood analysis results for the LP and PL models in a $TS_{\rm LP} = 677$ and $TS_{\rm PL} = 660$, respectively. The corresponding curvature test statistic is $TS_{\rm curve} = 17$, which corresponds to a significance of $\sim 4.3\sigma$. This indicates that the LP is preferred over a simple PL for this time interval, in agreement with the results obtained for the observations during 2008 August–2010 August (Nolan et al. 2012).

Fig. 1 shows the γ-ray light curve for the period 2012 December 1–2013 January 31 using an LP model and 1-week time bins. For the highest significance periods, we also reported fluxes in 1-d time intervals. For each time bin, the spectral parameters for PMN J0948+0022 and for all the sources within 10° from the target were frozen to the value resulting from the likelihood analysis over the whole period. If TS $<$ 10, 2σ upper limits were calculated. All uncertainties in measured γ-ray flux reported throughout this paper are statistical only. The systematic uncertainty on the effective area amounts to 10 per cent below 100 MeV, decreasing linearly with the logarithm of energy to 5 per cent between 316 MeV and 10 GeV, and increasing linearly with the logarithm of energy up to 15 per cent at 1 TeV (Ackermann et al. 2012).

During the period of high activity (2012 December 15–2013 January 11; MJD 56276–56303), the fit with an LP model in the 0.1–100 GeV energy range results in a TS = 410, with an average flux of $(46.8 \pm 4.7) \times 10^{-8}$ ph cm^{-2} s^{-1}, a spectral slope of $\alpha = 2.37 \pm 0.10$ at the reference energy $E_0 = 271$ MeV, and a curvature parameter $\beta = 0.10 \pm 0.04$. This suggests marginal spectral variability during the γ-ray flaring activity with respect to the whole period. The emission peak was observed on 2013 January 1 (MJD 56293), with an average flux for that day of $(155 \pm 31) \times 10^{-8}$ ph cm^{-2} s^{-1} in the 0.1–100 GeV energy range, corresponding to an apparent isotropic γ-ray luminosity of $\sim 1.5 \times 10^{48}$ erg s^{-1}. This is the highest flux observed from PMN J0948+0022 so far in γ-rays (see Foschini et al. 2012).

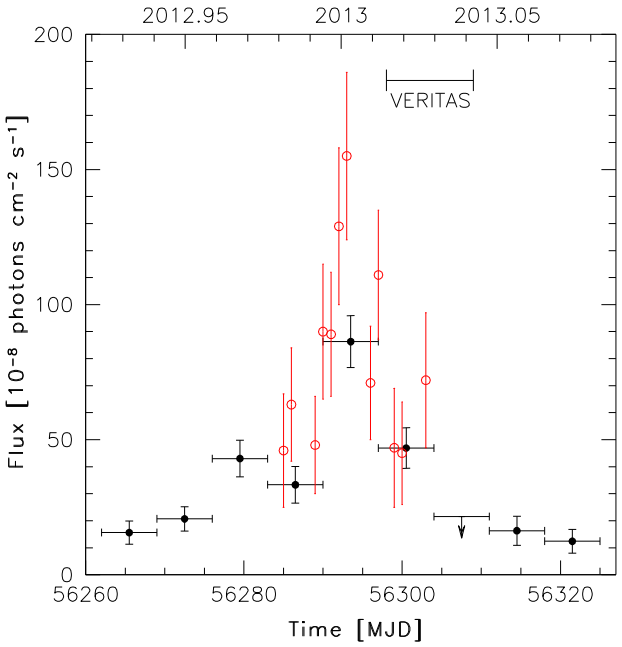

Figure 1. Integrated flux light curve of PMN J0948+0022 obtained by *Fermi*-LAT in the 0.1–100 GeV energy range during 2012 December 1–2013 January 31 with 7-d time bins. Arrow refers to 2σ upper limits on the source flux. Upper limits are computed when TS $<$ 10. Open circles represent daily fluxes reported for the periods of high activity. No upper limits are shown for daily data. The horizontal line indicates the period of the VERITAS observation.

By means of the `gtsrcprob` tool and using the source model optimized over the period 2012 December–2013 August, we estimated that the highest energy photon detected from PMN J0948+0022 was observed on 2013 January 5 at a distance of 0.°06 from the source with a probability of 98.5 per cent to be associated with the target and an energy of 7.2 GeV. Analysing the LAT data collected over the whole period in the 1–100 GeV energy range with a simple PL, the fit yielded a TS = 143, with a photon index of $\Gamma_\gamma = 2.64 \pm 0.19$ and an average flux of $(3.4 \pm 0.5) \times 10^{-9}$ ph cm^{-2} s^{-1}. On the contrary, the source is not detected at $E > 10$ GeV (TS = 1) with a 2σ upper limit of 1.5×10^{-10} ph cm^{-2} s^{-1} (assuming a photon index $\Gamma_\gamma = 3$).

3 VERITAS DATA: ANALYSIS AND RESULTS

The VERITAS observatory (Holder et al. 2006, 2008) is an array of four imaging atmospheric Cherenkov telescopes (IACT) located at the Fred Lawrence Whipple Observatory near Tucson, Arizona. Each telescope consists of a 12 m diameter reflector and a photomultiplier camera covering a field of view of 3.°5. The array has an effective area of $\sim 5 \times 10^4$ m^2 between 0.2 and 10 TeV.

VERITAS can detect a source with 2–3 per cent of the Crab nebula flux[6] in 300 min of exposure, with improved sensitivity to soft-spectrum sources following an update of the camera photomultipliers in Summer 2012 (Kieda et al. 2013). The angular and energy resolution for reconstructed γ-ray showers are 0.°1 and 15 per cent, respectively, at 1 TeV.

[6] 1 Crab = 2.1×10^{-10} ph cm^{-2} s^{-1} for $E > 200$ GeV (Hillas et al. 1998).

Table 1. VERITAS observations and results of PMN J0948+0022.

Date (MJD)	Date (UT)	Exposure (min)	Significance (σ)	N_{ex}	$F_{>0.2\,TeV}$ (10^{-11} ph cm^{-2} s^{-1})
56298	2013-01-06	33	−1.2	-9.8	<0.84
56299	2013-01-07	77	−0.3	-3.3	<0.54
56301	2013-01-09	75	1.1	15.0	<1.12
56305	2013-01-13	25	0.0	−0.1	<1.22
56306	2013-01-14	17	0.0	0.0	<1.53
56307	2013-01-15	13	1.9	10.6	<4.58
56308	2013-01-16	50	0.3	3.0	<1.08
56309	2013-01-17	25	−1.2	−8.8	<2.22
All data	–	315	0.4	10.6	<0.40

After a trigger from *Fermi*-LAT (D'Ammando & Orienti 2013), VERITAS observations of PMN J0948+0022 took place between 2013 January 6 (MJD 56298) and January 17 (MJD 56309), covering the decay of the γ-ray flare. Observations consisted of 30 min exposures pointing 0.°5 offset in *wobble* observing mode (Fomin et al. 1994) at a median zenith angle of 32°. About one-third of the collected data had to be rejected because of cloud coverage, leaving an effective dead-time corrected exposure of 315 min.

A description of the VERITAS analysis can be found in Acciari et al. (2008) and Archambault et al. (2013). To ensure a robust estimation of the shower parameters, at least two telescope images with a total signal size equivalent to >74 photoelectrons were required for an event to be reconstructed. Background-rejection cuts, optimized for a moderately bright soft-spectrum source, were applied to remove over 99.9 per cent of the charged cosmic rays. Events with reconstructed arrival direction $\theta < 0.^{\circ}1$ to the position of PMN J0948+0022 were selected as signal. The number of background events in the signal region was estimated from off-source regions in the same field of view using the *reflected region* technique (Berge, Funk & Hinton 2007).

The analysis revealed no significant γ-ray signal from PMN J0948+0022. An excess (N_{ex}) of 11 candidate γ-ray events over a background of 615 was measured, corresponding to a significance of 0.4 standard deviations according to equation 17 in Li & Ma (1983), with $N_{on} = 626$, $N_{off} = 5211$, and a ratio of the on-source time to the off-source time $\alpha = 0.118$. Assuming a PL spectrum with photon index $\Gamma_\gamma = 3.5$, a 99 per cent confidence level (c.l.) flux upper limit of $F_{>0.2\,TeV} < 4.0 \times 10^{-12}$ ph cm^{-2} s^{-1} was derived using the prescription by Rolke, López & Conrad (2005). The systematic uncertainty in the flux measurement is approximately 40 per cent. Differential upper limits (95 per cent c.l., $\Gamma_\gamma = 3.5$ to match the LAT spectrum during the period of high activity) at the energy threshold of the analysis (170 GeV) and where the correlation between flux level and spectral shape is minimal (300 GeV) are shown in Fig. 3. Compatible results were obtained using an independent analysis package with a different set of event-selection cuts.

Given the variable nature of the γ-ray emission from PMN J0948+0022, a search for signal in nightly bins (Table 1) as well as in 30-min runs was also conducted. However, no significant γ-ray excess was found at those time-scales either.

4 X-RAY TO OPTICAL DATA

4.1 *Swift* data analysis

The *Swift* satellite (Gehrels et al. 2004) performed six observations of PMN J0948+0022 between 2012 December and 2013 January. The observations were carried out with all three instruments on board: the X-ray Telescope (XRT; Burrows et al. 2005, 0.2–10.0 keV), the Ultraviolet/Optical Telescope (UVOT; Roming et al. 2005, 170–600 nm) and the Burst Alert Telescope (BAT; Barthelmy et al. 2005, 15–150 keV). The hard X-ray flux of this source is below the sensitivity of the BAT instrument for the short exposures of these observations; therefore, the data from this instrument are not used. Moreover, the source was not present in the *Swift* BAT 70-month hard X-ray catalogue (Baumgartner et al. 2013).

The XRT data were processed with standard procedures (`xrtpipeline v0.12.8`), filtering, and screening criteria using the HEASOFT package (v6.13). The data were collected in photon counting mode for all of the observations. The source count rate was low (<0.5 counts s^{-1}); thus, pile-up correction was not required. Source events were extracted from a circular region with a radius of 20 pixels (1 pixel = 2.36 arcsec), while background events were extracted from a circular region with radius of 50 pixels away from the source region and from other bright sources. Ancillary response files were generated with `xrtmkarf`, and account for different extraction regions, vignetting and point spread function corrections. We used the spectral redistribution matrices v013 in the Calibration data base maintained by HEASARC.[7] The spectra with low numbers of photons collected (<200 counts) were rebinned with a minimum of 1 count per bin and the Cash statistic (Cash 1979) was used. We fitted the spectra with an absorbed PL using the photoelectric absorption model `tbabs` (Wilms, Allen & McCray 2000), with a neutral hydrogen column density fixed to its Galactic value (5.07×10^{20} cm^{-2}; Kalberla et al. 2005). The fit results are reported in Table 2, and the 0.3–10 keV fluxes are shown in Fig. 2.

UVOT data in the v, b, u, $w1$, $m2$, and $w2$ filters were reduced with the HEASOFT package v6.13 and the 20120606 CALDB-UVOTA release. We extracted the source counts from a circle with 5 arcsec radius centred on the source and the background counts from a circle with 10 arcsec radius in a nearby source-free region. The observed magnitudes are reported in Table 3. As in, e.g., Raiteri et al. (2011), we calculated the effective wavelengths, count-to-flux conversion factors (CF_Λ), and amount of Galactic extinction in the UVOT bands (A_Λ) by convolving the mean Galactic extinction law by Cardelli, Clayton & Mathis (1989) with a PL fit to the source flux and with the filter effective areas. To obtain the UVOT de-reddened fluxes, we multiplied the count rates for the CF_Λ and corrected for the corresponding Galactic extinction values A_Λ. The UVOT density fluxes are reported in Fig 2.

[7] http://heasarc.nasa.gov/

Table 2. Log and fitting results of *Swift*–XRT observations of PMN J0948+0022 using a PL model with an H I column density fixed to the Galactic value in the direction of the source.

Date (MJD)	Date (UT)	Net exposure time (s)	Photon index (Γ_X)	Flux 0.3–10 keV[a] (10^{-12} erg cm^{-2} s^{-1})
56264	2012-12-03	1963	1.53 ± 0.25	3.3 ± 0.5
56286	2012-12-25	1893	1.51 ± 0.21	5.1 ± 0.5
56291	2012-12-30	722	1.77 ± 0.16	13.6 ± 1.3
56295	2013-01-03	2972	1.48 ± 0.15	6.8 ± 0.5
56303	2013-01-11	2932	1.60 ± 0.17	6.9 ± 0.6
56309	2013-01-17	3284	1.67 ± 0.10	10.6 ± 0.6

[a]Unabsorbed flux.

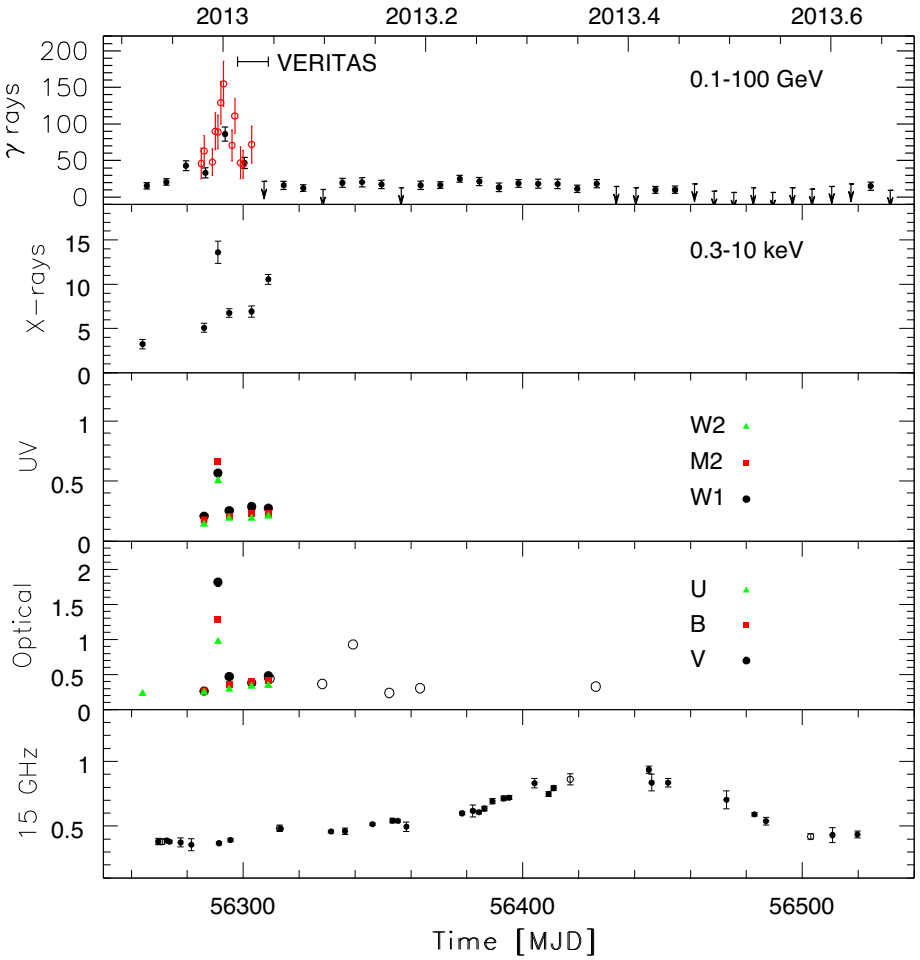

Figure 2. Multifrequency light curve for PMN J0948+0022. The period covered is 2012 December 1–2013 August 31 (MJD 56262–56535). The data were collected (from top to bottom) by *Fermi*-LAT (γ-rays; in units of 10^{-8} ph cm^{-2} s^{-1}), *Swift*-XRT (0.3–10 keV; in units of 10^{-12} erg cm^{-2} s^{-1}), *Swift*-UVOT ($w1$, $m2$, and $w2$ filters; in units of mJy), CRTS (open circles; in units of mJy) and *Swift*-UVOT (v, b, and u filters; in units of mJy), MOJAVE (open circles), and OVRO (15 GHz; in units of Jy). The horizontal line in the top panel indicates the period of the VERITAS observation.

Table 3. Results of the *Swift*-UVOT observations of PMN J0948+0022 in magnitudes.

Date (MJD)	Date (UT)	v	b	u	$w1$	$m2$	$w2$
56264	2012-12-03	–	–	17.43 ± 0.03	–	–	–
56286	2012-12-25	18.11 ± 0.18	18.29 ± 0.10	17.34 ± 0.07	17.29 ± 0.07	17.46 ± 0.05	17.46 ± 0.04
56291	2012-12-30	16.01 ± 0.10	16.59 ± 0.07	15.86 ± 0.06	16.20 ± 0.04	15.88 ± 0.08	16.08 ± 0.05
56295	2013-01-03	17.48 ± 0.09	18.00 ± 0.07	17.19 ± 0.06	17.07 ± 0.05	17.16 ± 0.06	17.12 ± 0.04
56303	2013-01-11	17.70 ± 0.11	17.85 ± 0.06	17.02 ± 0.05	16.94 ± 0.05	17.01 ± 0.05	17.14 ± 0.04
56309	2013-01-17	17.45 ± 0.09	17.81 ± 0.06	16.99 ± 0.05	17.00 ± 0.05	17.02 ± 0.05	17.04 ± 0.04

4.2 CRTS data

The source has been monitored by the CRTS (Drake et al. 2009; Djorgovski et al. 2011), using the 0.68 m Schmidt telescope at Catalina Station, AZ, and an unfiltered CCD. The typical cadence is four exposures separated by 10 min in a given night; this may be repeated up to four times per lunation, over a period of ∼6–7 months each year, while the field is observable. Photometry is obtained using the standard Source-Extractor package (Bertin & Arnouts 1996) and transformed from the unfiltered instrumental magnitude to Cousins V[8] by $V = V_{\rm CSS} + 0.31(B - V)^2 + 0.04$. We averaged the values obtained during the same observing night. The flux densities collected by CRTS in the V band are reported in Fig. 2.

5 RADIO DATA

5.1 OVRO data analysis

As part of an ongoing blazar monitoring programme, the OVRO 40 m radio telescope has observed PMN J0948+0022 at 15 GHz regularly since the end of 2007 (Richards et al. 2011). This monitoring programme includes about 1700 known and likely γ-ray loud blazars above declination -20°. The sources in this programme are observed in total intensity twice per week with a 4 mJy (minimum) and 3 per cent (typical) uncertainty on the flux densities. Observations were performed with a dual-beam (each 2.5 arcmin FWHM) Dicke-switched system using cold sky in the off-source beam as the reference. Additionally, the source is switched between beams to reduce atmospheric variations. The absolute flux density scale is calibrated using observations of 3C 286, adopting the flux density (3.44 Jy) from Baars et al. (1977). This results in about a 5 per cent absolute scale uncertainty, which is not reflected in the plotted errors.

5.2 MOJAVE data analysis

We investigated the parsec-scale morphology and flux density variability at 15 GHz by means of 6-epoch Very Long Baseline Array data from the MOJAVE programme (Lister et al. 2009). The data sets span the time interval between 2012 July and 2013 July, in order to overlap with the *Fermi*-LAT data. We imported the calibrated *uv* data into the National Radio Astronomy Observatory AIPS package. In addition to the total intensity images, we produced the Stokes Q and U images, to derive information on the polarized emission. The flux density was derived by means of the AIPS task JMFIT which performs a Gaussian fit on the image plane. Total intensity flux density and polarization information are reported in Table 4. The uncertainties on the flux density scale are less than 5 per cent, and the errors on the polarization angle are ∼5° (Lister et al. 2013).

Table 4. Flux density and polarization of PMN J0948+0022 from 15 GHz MOJAVE data.

Date (MJD)	Date (UT)	$S_{\rm Core}$[a] (mJy)	$S_{\rm Jet}$[a] (mJy)	$S_{\rm pol}$[a] (mJy) (per cent)	EVPA[b] (deg)
56120	2012-07-12	325	5	3 (0.9 per cent)	96
56242	2012-11-11	336	5	3 (0.9 per cent)	86
56271	2012-12-10	380	6	4 (1.0 per cent)	97
56313	2013-01-21	483	4	3 (0.6 per cent)	130
56417	2013-05-05	862	5	6 (0.7 per cent)	96
56503	2013-07-30	420	3	12 (2.9 per cent)	90

[a]Uncertainties on the flux densities are less than 5 per cent.
[b]Uncertainties on the polarization angles are 5°.

6 DISCUSSION

6.1 Radio to γ-ray behaviour

During 2012 December–2013 January, the NLSy1 PMN J0948+0022 showed new flaring activity in γ-rays, triggering follow-up observations by *Swift* and VERITAS. In Fig. 2, we compare the γ-ray light curve collected by *Fermi*-LAT in the 0.1–100 GeV energy range with the X-ray (0.3–10 keV), UV ($w1$, $m2$, and $w2$ filters), optical (v, b, and u filters), and radio (15 GHz) light curves collected by *Swift* (XRT and UVOT), CRTS, MOJAVE, and OVRO.

The γ-ray flaring period peaked on 2013 January 1 (MJD 56293) with a variability amplitude (calculated as the ratio between the maximum and minimum flux) of ∼15 between 2012 December and 2013 August, and flux variations on a daily time-scale. The peak flux reported here, $(155 \pm 31) \times 10^{-8}$ ph cm^{-2} s^{-1}, is the greatest detected from this source so far at γ-rays (see e.g. Foschini et al. 2012). The γ-ray flaring activity ended in 2013 mid-January, and no further significant increase of the γ-ray flux was observed up to 2013 August. Only marginal spectral variability was observed during this flaring activity, similar to the behaviour shown in Foschini et al. (2012) for the period 2008 August–2011 December.

During the highest γ-ray activity, a quasi-simultaneous increase was observed from optical to X-rays. *Swift*/XRT observed the source with a 0.3–10 keV flux in the range $(3.3–13.6) \times 10^{-12}$ erg cm^{-2} s^{-1}, with a variability amplitude of ∼4 (Table 2). The peak of the X-ray flux was observed on 2012 December 30 (MJD 56291), when the source reached the highest flux detected for this source so far (for a comparison, see Foschini et al. 2012; D'Ammando et al. 2014). No significant spectral change in the X-ray band was observed during the *Swift* observations, with the photon index ranging between 1.5 and 1.8, similarly to what was observed in 2011 (D'Ammando et al. 2014). It is worth mentioning that a second increase of the X-ray flux was observed on 2013 January 17 (MJD 56309), but no corresponding increase of activity was observed in γ-ray, UV, and optical bands.

The optical and UV emission significantly increased over only 5 d, from 2012 December 25 (MJD 56286) to December 30 (MJD 56291), suggesting that the dominant contribution to the continuum flux should come from the synchrotron emission. However, the variability amplitude decreases with frequency: from ∼7 in the V band to ∼3.5 in the UV part of the spectrum. This could be due to the contribution in UV of the thermal emission from the accretion disc, which is well identified during low-activity periods of this source (Foschini et al. 2012). A similar behaviour was already noticed in some FSRQs (e.g. 3C 454.3; Raiteri et al. 2011). After the γ-ray flare, two observations were performed in the V band by the Steward Observatory as part of the blazar monitoring programme of the University of Arizona.[9] Optical polarization of 4.0 ± 0.1 and 1.1 ± 0.1 per cent was estimated on 2013 January 17 and 18, respectively, while the position angle on the sky of the linear polarization changed from $100^\circ \pm 1^\circ$ to $26^\circ \pm 3^\circ$. The value observed on 2013 January 17 is not as high as the 12.3 per cent observed for this source

[8] http://nesssi.cacr.caltech.edu/DataRelease/FAQ2.html#improve

[9] http://james.as.arizona.edu/~psmith/Fermi/

on 2013 May 25 (Eggen, Miller & Maune 2013), but the change of a factor of ∼4 in one day is notable as well as the significant change of the observed polarization angle. The rapid variation of optical polarization is a characteristic associated with the variation of synchrotron emission in blazars. The variation of both the fractional polarization and polarization angle may be an indication of a turbulent magnetic field (e.g. Marscher 2014).

PMN J0948+0022 was highly variable at 15 GHz during the OVRO 40 m telescope monitoring, with the flux density varying from 357 mJy (on MJD 56281; 2012 December 20) to 936 mJy (on MJD 56445; 2013 June 2), as shown in Fig. 2. The source was observed in a low state at 15 GHz during the peak of the γ-ray activity. On the other hand, no significant γ-ray activity was detected at the time of the peak of the radio activity. If the γ-ray and radio activity are connected, the observed peak at 15 GHz is produced by the same disturbance of the jet responsible for the γ-ray flare delayed by ∼5 months. This delay may be explained by synchrotron self-absorption opacity effects in combination with shock propagation effects. As an alternative, the γ-ray and radio emission may originate in different parts of a bending and inhomogeneous jet, with variable orientations with respect to the line of sight. Therefore, we may have different Doppler boosting of the zone responsible for the optical-to-γ-ray emission and that responsible for the radio emission in the two flaring periods (e.g. Raiteri et al. 2012). A delay of ∼50 d of the 15 GHz flux density peak with respect to the γ-ray one was observed during the 2010 γ-ray flaring activity of PMN J0948+0022 (Foschini et al. 2011). On the contrary, no obvious connection between γ and radio emission was observed in 2011 (D'Ammando et al. 2014). The lack of a coherent pattern suggests a complex connection between the radio and γ-ray emission for PMN J0948+0022, as also observed in the other NLSy1 SBS 0846+513 (D'Ammando et al. 2013b, 2012) as well as in blazars (e.g. PKS 1510−089; Orienti et al. 2013).

At pc-scales the radio emission is dominated by the core component, which accounts for ∼98 per cent of the total emission. A hint of the jet emerges from the core with a position angle ∼30°, consistent with what was found in previous works (e.g. Giroletti et al. 2011; D'Ammando et al. 2014). From the pc-scale resolution images, we can separate the core flux density from the jet emission, in order to study the light curve and polarization properties of each of them. In accordance with the OVRO monitoring, the flux density of the core observed by MOJAVE at 15 GHz increased from 2012 July 12 to 2013 May 5, when a value of 862 mJy was reached (Table 4). No significant increase of the flux density from the jet was observed. A higher polarized emission of the core ($S_{\rm pol}$) and polarization percentage were observed on 2013 July 30, after the peak of the radio emission. The electric vector position angle (EVPA) of the core shows a moderate change during the MOJAVE observation, ranging from 86° to 130°, similar to what was observed for the same object in 2011 (D'Ammando et al. 2014). In particular, we noted a change of ∼25° between 2012 December and 2013 January, after the γ-ray flare observed by LAT.

Because γ-ray emission from NLSy1s was not expected until its discovery with the *Fermi* satellite, no dedicated observations of these sources were carried out at VHE before that time. The detection of a few of these objects in γ-rays by the LAT has given rise to a new interest in their emission processes at the higher energies. The only γ-ray emitting NLSy1 with VHE observations in the literature is 1H 0323+342 ($z = 0.062$), which was selected from a list of candidate TeV-emitting FSRQs (Perlman 2000). It was observed by the Whipple telescope during 2001–2003, resulting in an upper limit of 5.2×10^{-12} ph cm^{-2} s^{-1} above 400 GeV, with marginal

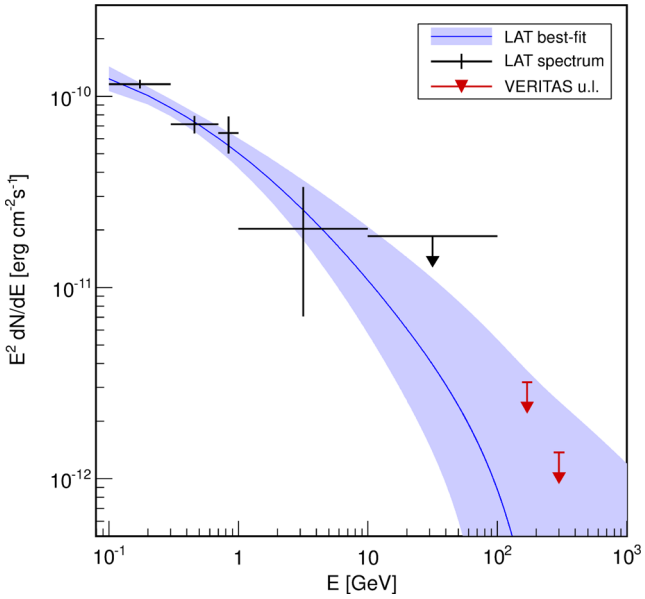

Figure 3. SED of PMN J0948+0022 in the MeV-to-TeV energy range. The *Fermi*-LAT spectrum was extrapolated to the TeV energies and corrected for EBL absorption using the model of Finke et al. (2010). *Fermi*-LAT and VERITAS data points and upper limits are shown. VERITAS upper limits are calculated at the energy threshold of the analysis and where the correlation between flux level and spectral shape is minimal.

evidence of a rate increase in the 2001–2002 light curve (Falcone et al. 2004). This paper provides the first report of an observation of an NLSy1 with the current generation of IACTs (i.e. VERITAS, MAGIC, and HESS). Unfortunately, the source was not detected by VERITAS at VHE in 2013 January, with an upper limit of 4.0×10^{-12} ph cm^{-2} s^{-1} above 200 GeV. This could be due to several reasons. First of all, the distance of the source is relatively large ($z = 0.5846$), and so most of the GeV/TeV emission should be absorbed due to pair production from γ-ray photons of the source and the infrared photons from the extragalactic background light (EBL), although the most distant FSRQ detected at VHE, 3C 279 (Albert et al. 2008), is at a comparable distance of $z = 0.5362$. Considering the Finke, Razzaque & Dermer (2010) model for the EBL the optical depth is $\tau \sim 1$ for 170 GeV photons at $z = 0.5846$. As a comparison, using the Dominguez et al. (2011) model the optical depth is $\tau \sim 1$ for 200 GeV photons at the same distance. However, the VERITAS observations were carried out a few days after the peak of the γ-ray activity from PMN J0948+0022 detected by LAT, thus covering only the last part of the MeV–GeV flare. An extrapolation to the VHE band of the LAT measured energy spectrum averaged over the active phase of the flare (2012 December 29–2013 January 18) falls below the VERITAS sensitivity in 5 h of observation once the EBL absorption is taken into account (Fig. 3). Assuming no additional spectral curvature than that already seen in the LAT energy range (LP with $\beta = 0.1$) and the flux suppression induced by the EBL, detectable VHE emission from PMN J0948+0022 would be expected during GeV flares with $F_{0.1-100\,\rm GeV} \geq 2 \times 10^{-6}$ ph cm^{-2} s^{-1}. Given the similarities between PMN J0948+0022 and γ-ray-detected FSRQs, the presence of a bright broad-line region (BLR) could produce a spectral break due to pair production, suppressing the flux beyond a few GeV and preventing a VHE detection. However, the role of BLR photons in the emission/absorption of VHE γ-rays is far from understood, and the detections of the FSRQ 3C 279 (Albert et al. 2008), 4C +21.35

(Aleksić et al. 2011), and PKS 1510-089 (Abramowski et al. 2013) have shown that the spectrum of some FSRQs extends to VHE energies during certain flaring periods. This may be an indication that during those high-activity periods the γ-ray emission was produced outside the BLR.

6.2 SED modelling

We created two SEDs for comparing the 2013 January γ-ray flaring activity (presented in this paper) to the 2011 May intermediate state (presented in D'Ammando et al. 2014). The 2013 flaring SED includes the LAT spectrum built with data centred on 2012 December 29–2013 January 18 (MJD 56290–56310), optical, UV, and X-ray data collected by *Swift* (XRT and UVOT) on 2012 December 30 (MJD 56291), and radio data collected by OVRO at 15 GHz on 2013 January 3 (MJD 56295). The 2011 intermediate SED was built with LAT data centred on 2011 May 22–June 11 (MJD 55703–55723), optical, UV, and X-ray data collected by *XMM–Newton* [European Photon Imaging Camera (EPIC) and Optical Monitor] on 2011 May 28–29 (MJD 55709–55710), and radio data collected by Effelsberg at 15 and 32 GHz on 2011 May 24 (MJD 55705).

The location along the jet of the γ-ray emitting region is controversial; see the discussion by Finke (2013b). Rapid variability (Tavecchio et al. 2010; Brown 2013; Saito et al. 2013) indicates a compact emitting region that, if the emitting region takes up the entire cross-section of the jet, argues for emission from inside the BLR. Absorption features in γ-ray spectra could also be an indication of this (Poutanen & Stern 2010; Stern & Poutanen 2011, 2014). On the other hand, γ-ray spectra that extend to VHEs without absorption features in some objects (Aleksić et al. 2011, 2014; Pacciani et al. 2014) are a strong indication that emission takes place outside the BLR, where the dust torus is likely the dominant external radiation field. This is corroborated by the association of γ-ray flares with the radio outbursts and the ejection of superluminal components from cores of blazars as observed with very long baseline interferometry, giving distances $\gtrsim$ a few pc based on light travel time arguments (e.g. Marscher et al. 2010; Orienti et al. 2013). There is some indication that different flares, even from the same source, can occur in different locations (Brown 2013; Nalewajko, Begelman & Sikora 2014). Equipartition arguments can also be invoked for locating the emitting region (Dermer et al. 2014). In the following, we first model the emitting region consistent with a dust torus external radiation field, then discuss modelling consistent with an emitting region inside the BLR.

We modelled the SED of the two activity states of PMN J0948+0022 with a combination of synchrotron, synchrotron self-Compton (SSC), and external Compton (EC) non-thermal emission. The synchrotron component considered is self-absorbed below 10^{11} Hz and thus cannot reproduce the radio emission. This emission is likely from the superposition of multiple self-absorbed jet components (Königl 1981). We also included thermal emission by an accretion disc and dust torus. The modelling details can be found in Finke, Dermer & Böttcher (2008) and Dermer et al. (2009). Additionally, a soft excess was observed in the X-ray spectrum during the 2011 state, whose origin is still under debate (D'Ammando et al. 2014). In order to account for the soft X-ray excess in the 2011 SED, we included emission from the disc which is Compton scattered by an optically thin thermal plasma near the accretion disc (i.e. a corona). This was done using the routine '`SIMPL`' (Steiner et al. 2009). This routine has two free parameters: the fraction of disc photons scattered by the corona ($f_{\rm sc}$), and the PL photon index of the scattered coronal emission ($\Gamma_{\rm sc}$). The mass of the black hole (BH) was chosen to be the same as the one used by Foschini et al. (2011), $M_{\rm BH} = 1.5 \times 10^8$ M$_\odot$, consistent with estimates by Zhou et al. (2003) and Abdo et al. (2009a).

The observed variability time-scale of $\sim$1 d (Fig. 1) constrains the size of the emitting region, consistent with the γ-ray light curve (Fig. 2). The results of the modelling can be found in Table 5 and Fig. 4 (for a description of the model parameters, see Dermer et al. 2009). Both models have the jet power in magnetic field about a factor of 10 above the jet power in electrons.[10] However, it is possible that the combined power in electrons and protons in the jet could be in equipartition with the magnetic field. If this is the case, it implies that the jet power in protons is $P_{\rm j,\,p} \approx 4.8 \times 10^{45}$ erg s^{-1} from the 2011 model and $P_{\rm j,\,p} \approx 1.9 \times 10^{46}$ erg s^{-1} from the 2013 flaring model. This model assumes that the emitting region is outside the BLR, where dust torus photons are likely the seed photon source. This source was modelled as being an isotropic, monochromatic radiation source with dust parameters chosen to be consistent with the relation between inner radius, disc luminosity, and dust temperature from Nenkova et al. (2008). Note that the model parameters shown here are not unique, and other model parameters could also reproduce the SED, especially for the 2011 state.

In 2011 May–June, the γ-ray and X-ray flux was intermediate between the 2013 flaring activity and the low-activity state observed e.g. in 2009 May 15 (Foschini et al. 2012), with no corresponding flare in the optical. This aspect and the shape of the optical spectrum indicate that the optical emission during that period was dominated by thermal accretion disc emission. The synchrotron component was poorly constrained, other than an upper limit from the optical data. According to our model, thermal emission from the dust torus would be visible if infrared observations were available. The X-rays originated from a combination of coronal emission (for the soft excess) and EC emission. In this model, the SSC emission was quite weak and did not play a significant role in the SED.

The 2013 activity state was brighter across the electromagnetic spectrum than during 2011. In particular, the 2013 flaring period included a flare in optical as well as in X-rays and γ-rays. The much stronger optical emission implies that the two activity states differed by more than just the electron distribution. This is in contrast to the FSRQ PKS 0537−441, where high- and low-activity states were modelled by only changing the electron distribution (D'Ammando et al. 2013a). In this way, PMN J0948+0022 is similar to the FSRQ PKS 2142−75 (Dutka et al. 2013), which exhibited multiple flares where another parameter besides the electron distribution needed to be changed between flares. As for PKS 2142−75, we modelled the two activity states of PMN J0948+0022 by changing the magnetic field and the electron distribution. This may be an indication that the shock responsible for the flare produces a compression as it passes through the emitting region yielding an amplification of the magnetic field during the flare. The 2011 intermediate state from PMN J0948+0022 is similar to 'flare B' from PKS 2142−75 (Dutka et al. 2013), since in both cases the optical part of the spectrum is dominated by the thermal disc emission. The 2013 flare from PMN J0948+0022 is most like 'flare A' from PKS 2142−75 (Dutka et al. 2013), since for both of these flares the optical spectrum of the two sources is dominated by non-thermal synchrotron emission. We also modelled the 2013 flaring state with parameters consistent with Compton-scattering of BLR Hα (6563 Å) line radiation; again, see

[10] Jet powers were calculated assuming a two-sided jet. See Finke et al. (2008).

Table 5. Model parameters for the SEDs shown in Fig. 4.

Parameter	Symbol	2011 intermediate	2013 flare (dust torus)	2013 flare (BLR)
Redshift	z	0.585	0.585	0.585
Bulk Lorentz factor	Γ	30	30	12
Doppler factor	$\delta_{\rm D}$	30	30	12
Magnetic field (G)	B	0.5	1.0	1.0
Variability time-scale (s)	$t_{\rm v}$	10^5	10^5	10^5
Comoving radius of blob (cm)	$R'_{\rm b}$	5.7×10^{16}	5.7×10^{16}	2.3×10^{16}
Low-energy electron spectral index	p_1	2.5	2.35	2.35
High-energy electron spectral index	p_2	4.0	4.0	3.9
Minimum electron Lorentz factor	$\gamma'_{\rm min}$	2.7	1.0	1.0
Break electron Lorentz factor	$\gamma'_{\rm brk}$	5.0×10^2	6.8×10^2	7.8×10^2
Maximum electron Lorentz factor	$\gamma'_{\rm max}$	1.0×10^4	1.0×10^4	1.0×10^4
Black hole mass ($M_\odot$)	$M_{\rm BH}$	1.5×10^8	1.5×10^8	1.5×10^8
Disc luminosity (erg s^{-1})	$L_{\rm disc}$	5.7×10^{45}	5.7×10^{45}	5.7×10^{45}
Inner disc radius ($R_{\rm g}$)	$R_{\rm in}$	6.0	6.0	6.0
Accretion efficiency	$\eta_{\rm disc}$	1/12	1/12	1/12
Fraction of photons scattered by corona	$f_{\rm sc}$	0.35	0.35	0.35
Photon index of scattered coronal emission	$\Gamma_{\rm sc}$	2.3	2.3	2.3
Seed photon source energy density (erg cm^{-3})	$u_{\rm seed}$	2.0×10^{-4}	2.0×10^{-4}	0.3
Seed photon source photon energy ($m_{\rm e}$ c^2)	$\epsilon_{\rm seed}$	7.0×10^{-7}	7.0×10^{-7}	3.7×10^{-6}
Dust torus luminosity (erg s^{-1})	$L_{\rm dust}$	1.1×10^{45}	1.1×10^{45}	1.1×10^{45}
Dust torus radius (cm)	$R_{\rm dust}$	3.8×10^{18}	3.8×10^{18}	3.8×10^{18}
Dust temperature (K)	$T_{\rm dust}$	1700	1700	1700
Jet power in magnetic field (erg s^{-1})	$P_{\rm j,\,B}$	5.4×10^{45}	2.2×10^{46}	5.5×10^{46}
Jet power in electrons (erg s^{-1})	$P_{\rm j,\,e}$	6.3×10^{44}	2.4×10^{45}	1.5×10^{44}

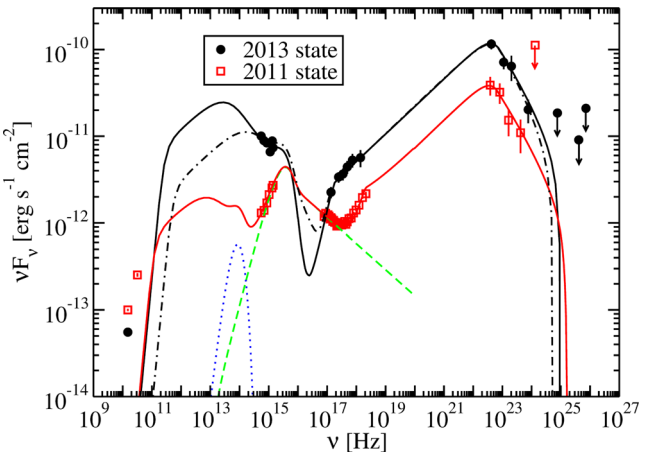

Figure 4. SEDs and models for the 2013 and 2011 activity states from PMN J0948+0022. The filled circles are the data from the 2013 flaring state, and the open squares are the data from the 2011 intermediate state taken from D'Ammando et al. (2014). The dashed curve indicates the disc and coronal emission, and the dotted line indicates the thermal dust emission. Solid lines represent models consistent with scattering dust torus radiation, while the dash–dotted curve represents a model consistent with the scattering of BLR Hα (6563 Å) radiation. Arrows refer to 2σ upper limits on the source flux. The VERITAS upper limits are corrected for EBL absorption using the model of Finke et al. (2010).

Fig. 4 and Table 5. The model reproduces the data approximately equally as well as the dust scattering model. Thus, it is not possible to distinguish between the two scenarios by snapshot spectral modelling. However, we note that the BLR scattering model is farther from equipartition, so this may be a weak argument in favour of the dust scattering scenario. As also observed in the NLSy1 SBS 0846+513 (D'Ammando et al. 2012), PMN J0948+0022 exhibits behaviour similar to other FSRQs. The X-ray emission is dominated by EC, and the coronal emission is not visible, so that there is no evidence for a soft excess from the data in 2013. However, this could be due to the low sensitivity of *Swift*-XRT at ∼1 keV.

A clear correlation between Compton dominance[11] and the rest-frame peak synchrotron frequency ($\nu^{\rm sy}_{\rm pk}$) for blazars was reported in Finke (2013a). This correlation is related to the contribution of the EC component, which results to be higher for larger values of Compton dominance. In Fig. 5, the Compton dominance versus $\nu^{\rm sy}_{\rm pk}$ is shown for sources from the second LAT AGN Catalogue (2LAC; Ackermann et al. 2011). In addition, we plot the low- and high-activity states of the NLSy1 SBS 0846+513 (D'Ammando et al. 2013b) and the intermediate- and high-activity states of PMN J0948+0022 shown in Fig. 4. Both NLSy1s are in a region occupied by FSRQs, indicating the similarity between FSRQs and these NLSy1s. It is worth mentioning that for both NLSy1s the peak frequency is higher for lower Compton dominances, in agreement with the general behaviour observed for blazars.

7 CONCLUSIONS

We reported on the observation by the *Fermi*-LAT of flaring γ-ray activity from the NLSy1 PMN J0948+0022 in 2012 December–2013 January. The γ-ray flux reached on 2013 January 1, $(155 \pm 31) \times 10^{-8}$ ph cm^{-2} s^{-1} in the 0.1–100 GeV energy range, is the highest value detected from this source and more generally from an NLSy1 so far. Only marginal spectral variability was observed in γ-rays during the flare. PMN J0948+0022 was not detected above $E >$ 10 GeV by LAT.

[11] Compton dominance is the ratio of the peak Compton luminosity to peak synchrotron luminosity.

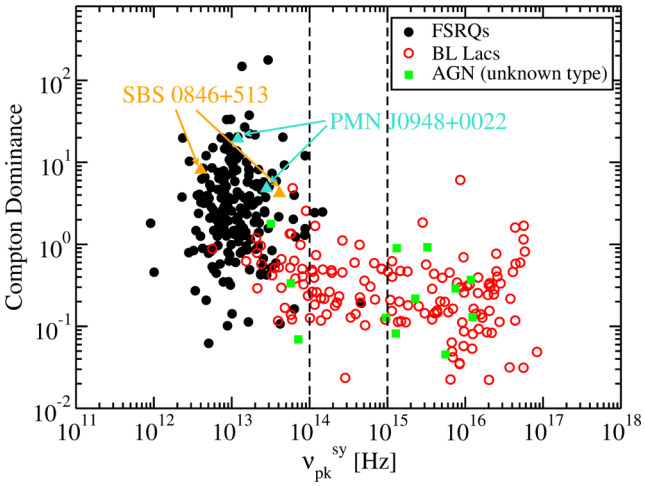

Figure 5. The Compton dominance versus peak synchrotron frequency for sources from the 2LAC (Ackermann et al. 2011), along with two states of SBS 0846+513 (D'Ammando et al. 2013b) and PMN J0948+0022 (this work). Filled circles represent FSRQs, open circles represent BL Lac objects, and filled squares represent AGN of unknown type. Adapted from Finke (2013a), PMN J0948+0022 and SBS 0846+513 are plotted as triangles.

We presented multiwavelength observations of the source from radio to VHE during the period 2012 December 1–2013 August 31 including data collected by VERITAS, *Fermi*-LAT, *Swift*, CRTS, MOJAVE, and OVRO. An intense flaring episode, quasi-simultaneous to the γ-ray one, was observed on 2012 December 30 in optical, UV, and X-rays, showing record flux also in these energy bands. This suggests a strict connection between the region responsible for the γ-ray activity and that responsible for the optical-to-X-ray activity, although the time sampling of the observations is too sparse from optical to X-rays to formally establish a correlation. Flaring activity was also observed at 15 GHz with the radio peak detected on 2013 June 2. The most likely scenario is that the radio flare is the delayed counterpart of the γ-ray one, with a delay of $\sim$5 months due to opacity effects and the propagation of the shock along the jet. Past flaring episodes from PMN J0948+0022 have shown a different delay or no indication of correlated variability (Foschini et al. 2011; D'Ammando et al. 2014), thus making the radio–gamma connection complex in this object. A slightly higher polarized emission from the core and polarization percentage was observed by MOJAVE after the peak of the radio emission, while no significant change of the EVPA was detected.

Following the γ-ray flare observed by the LAT, a first detection of VHE emission from PMN J0948+0022 was attempted by VERITAS. The observations carried out between 2013 January 6 and 17, just at the end of the γ-ray flaring activity, resulted in an upper limit of $F_{>0.2\,\mathrm{TeV}} < 4.0 \times 10^{-12}\,\mathrm{ph\,cm^{-2}\,s^{-1}}$. Further observations with the current generation of IACTs (VERITAS, MAGIC, and HESS), especially during the peak of γ-ray activity, may lead to VHE detections of this object. With a lower energy threshold and better sensitivity, future observations with the Cherenkov Telescope Array will constrain the level of γ-ray emission at 100 GeV and below (Sol et al. 2013). However, pair production due to the EBL significantly suppresses the VHE flux of PMN J0948+0022 given its redshift of 0.5846. 1H 0323+342 is another, closer ($z = 0.061$), NLyS1, already observed (but not significantly detected) at VHE during a search for TeV-emitting FSRQs (Falcone et al. 2004). If 1H 0323+342 exhibits flaring behaviour similar to that observed in PMN J0948+0022, then it will be a promising target for IACTs.

We compared the broad-band SED of the 2013 flaring activity state with that from an intermediate-activity state of PMN J0948+0022 observed in 2011. Contrary to what was observed for some FSRQs (e.g. PKS 0537−441; D'Ammando et al. 2013a), the two SEDs, modelled as an EC component of seed photons from a dust torus, could not be modelled by changing only the electron distribution parameters. A higher magnetic field is needed for modelling the high-activity state of PMN J0948+0022, as was also observed for the FSRQ PKS 2142−75 (Dutka et al. 2013). In a Compton dominance versus synchrotron peak frequency plot (see Fig. 5), the values for the two activity states of PMN J0948+0022 lie in the same region occupied by the FSRQs, as well as the other NLSy1 SBS 0846+513. This suggests that the EC scattering is likely the dominant mechanism for producing high-energy emission in PMN J0948+0022, confirming the similarities between γ-ray emitting NLSy1s and FSRQs. The inverse Compton (IC) peak of this source seems to lie at 100 MeV or below. With the improved sensitivity of the LAT at low energies with Pass 8 data (Atwood et al. 2013), we will be able to characterize in more detail the IC bump of PMN J0948+0022, and therefore the SED modelling.

In addition to the large uncertainties on the BH mass of the NLSy1 (e.g. Marconi et al. 2008; Calderone et al. 2013), the structure of the host galaxies is unclear. For four out of five NLSy1s detected in γ-rays by LAT, no high-resolution observations of their host galaxies are available. This is also related to the redshifts of these objects, and then the difficulty of detecting significant resolved structures for their host galaxies (e.g. SBS 0846+513; Maoz et al. 1993). Therefore, we cannot rule out the possibility that these γ-ray emitting NLSy1s are hosted in elliptical galaxies.

ACKNOWLEDGEMENTS

The *Fermi*–LAT Collaboration acknowledges generous ongoing support from a number of agencies and institutes that have supported both the development and the operation of the LAT as well as scientific data analysis. These include the National Aeronautics and Space Administration and the Department of Energy in the United States, the Commissariat à l'Energie Atomique and the Centre National de la Recherche Scientifique/Institut National de Physique Nucléaire et de Physique des Particules in France, the Agenzia Spaziale Italiana, and the Istituto Nazionale di Fisica Nucleare in Italy, the Ministry of Education, Culture, Sports, Science and Technology (MEXT), High Energy Accelerator Research Organization (KEK) and Japan Aerospace Exploration Agency (JAXA) in Japan, and the K. A. Wallenberg Foundation, the Swedish Research Council, and the Swedish National Space Board in Sweden. Additional support for science analysis during the operations phase is gratefully acknowledged from the Istituto Nazionale di Astrofisica in Italy and the Centre National d'Études Spatiales in France.

The VERITAS Collaboration is grateful to Trevor Weekes for his seminal contributions and leadership in the field of VHE gamma-ray astrophysics, which made this study possible. The work of the VERITAS Collaboration is supported by grants from the US Department of Energy Office of Science, the US National Science Foundation, and the Smithsonian Institution, by NSERC in Canada, by Science Foundation Ireland (SFI 10/RFP/AST2748) and by the Science and Technology Facilities Council in the UK. We acknowledge the excellent work of the technical support staff at the Fred Lawrence Whipple Observatory and at the collaborating institutions in the construction and operation of the instrument.

We thank the Swift team for making these observations possible, the duty scientists, and science planners. The OVRO 40 m

monitoring programme is supported in part by NASA grants NNX08AW31G and NNX11A043G, and NSF grants AST-0808050 and AST-1109911. The CRTS survey is supported by the US National Science Foundation under grants AST-0909182. This research has made use of data from the MOJAVE data base that is maintained by the MOJAVE team (Lister et al. 2009). Data from the Steward Observatory spectropolarimetric monitoring project were used. This programme is supported by Fermi Guest Investigator grants NNX08AW56G, NNX09AU10G, and NNX12AO93G. The National Radio Astronomy Observatory is a facility of the National Science Foundation operated under cooperative agreement by Associated Universities, Inc. We thank F. Schinzel, S. Digel, P. Bruel, and the referee, Anthony M. Brown, for useful comments and suggestions.

REFERENCES

Abdo A. A. et al., 2009a, ApJ, 699, 976
Abdo A. A. et al., 2009b, ApJ, 707, L142
Abdo A. A. et al., 2009c, ApJ, 707, 727
Abramowski A. et al., 2013, A&A, 554, A107
Acciari V. A. et al., 2008, ApJ, 679, 1427
Ackermann M. et al., 2011, ApJ, 743, 171
Ackermann M. et al., 2012, ApJS, 203, 4
Albert J. et al., 2008, Science, 320, 1752
Aleksić J. et al., 2011, ApJ, 730, L8
Aleksić J. et al., 2014, A&A, 569, A46
Archambault S. et al., 2013, ApJ, 776, 69
Atwood W. B. et al., 2009, ApJ, 697, 1071
Atwood W. B. et al., 2013, 2012 Fermi Symp. Proc. – eConf C121028, preprint (arXiv:1303.3514)
Baars J. W. M., Genzel R., Pauliny-Toth I. I. K., Witzel A., 1977, A&A, 61, 99
Barthelmy S. D. et al., 2005, Space Sci. Rev., 120, 143
Baumgartner W. H., Tueller J., Markwardt C. B., Skinner G. K., Barthelmy S., Mushotzky R. F., Evans P. A., Gehrels N., 2013, ApJS, 207, 19
Berge D., Funk S., Hinton J., 2007, A&A, 466, 1219
Bertin E., Arnouts S., 1996, A&AS, 117, 393
Brown A. M., 2013, MNRAS, 431, 824
Burrows D. N. et al., 2005, Space Sci. Rev., 120, 165
Calderone G., Ghisellini G., Colpi M., Dotti M., 2013, MNRAS, 431, 210
Cardelli J. A., Clayton G. C., Mathis J. S., 1989, ApJ, 345, 245
Carpenter B., Ohja R., 2013, Astron. Telegram, 5344
Cash W., 1979, ApJ, 228, 939
D'Ammando F., Ciprini S., 2011, Astron. Telegram, 3429
D'Ammando F., Orienti M., 2013, Astron. Telegram, 4694
D'Ammando F. et al., 2012, MNRAS, 426, 317
D'Ammando F. et al., 2013a, MNRAS, 431, 2481
D'Ammando F. et al., 2013b, MNRAS, 436, 191
D'Ammando F. et al., 2014, MNRAS, 438, 3521
Dermer C. D., Finke J. D., Krug H., Böttcher M., 2009, ApJ, 692, 32
Dermer C. D., Cerruti M., Lott B., Boisson C., Zech A., 2014, ApJ, 782, 82
Djorgovski S. G. et al., 2011, in Mihara T., Kawai N., eds, The First Year of MAXI: Monitoring Variable X-ray Sources. JAXA Special Publ., Tokyo, preprint (arXiv:1102.5004)
Dominguez A. et al., 2011, MNRAS, 410, 2556
Donato D., 2010, Astron. Telegram, 2733, 1
Donato D., 2011, Astron. Telegram, 3452, 1
Drake A. J. et al., 2009, ApJ, 696, 870
Dutka M. S. et al., 2013, ApJ, 779, 174
Eggen J. R., Miller H. R., Maune J. D., 2013, ApJ, 773, 85
Falcone A. D. et al., 2004, ApJ, 613, 710
Finke J. D., 2013a, ApJ, 763, 134
Finke J. D., 2013b, preprint (arXiv:1303.5095)
Finke J. D., Dermer C. D., Böttcher M., 2008, ApJ, 686, 181
Finke J. D., Razzaque S., Dermer C. D., 2010, ApJ, 712, 238
Fomin V. P., Stepanian A. A., Lamb R. C., Lewis D. A., Punch M., Weekes T. C., 1994, Astropart. Phys., 2, 137
Foschini L., 2010, Astron. Telegram, 2752
Foschini L. et al., 2011, MNRAS, 413, 1671
Foschini L. et al., 2012, A&A, 548, 106
Gehrels N. et al., 2004, ApJ, 611, 1005
Giroletti M. et al., 2011, A&A, 528, L11
Hillas A. M. et al., 1998, ApJ, 503, 744
Holder J. et al., 2006, Astropart. Phys., 25, 391
Holder J. et al., 2008, in Aharonian F. A., Hofmann W., Rieger F., eds, AIP Conf. Proc. Vol. 1085, High Energy Gamma-Ray Astronomy: Proceedings of the 4th International Meeting on High Energy Gamma-Ray Astronomy. Am. Inst. Phys., New York, p. 657
Kalberla P. M. W., Burton W. B., Hartmann D., Arnal E. M., Bajaja E., Morras R., Pöppel W. G. L., 2005, A&A, 440, 775
Kieda D. B. for the VERITAS Collaboration 2013, in Proc. 33rd Int. Cosmic Ray Conf., preprint (arXiv:1308.4849)
Konigl A., 1981, ApJ, 243, 700
Li T.-P., Ma Y.-Q., 1983, ApJ, 272, 317
Lister M. L. et al., 2009, AJ, 137, 3718
Lister M. L. et al., 2013, AJ, 146, 120
Maoz D., Bahcall J. N., Doxsey R., Schneider D. P., Bahcall N. A., Lahav O., Yanny B., 1993, ApJ, 402, 69
Marconi A., Axon D., Maiolino R., Nagao T., Pastorini G., Pietrini P., Robinson A., Torricelli G., 2008, ApJ, 678, 693
Marscher A. P., 2014, ApJ, 780, 87
Marscher A. P. et al., 2010, ApJ, 710, L126
Mattox J. R. et al., 1996, ApJ, 461, 396
Nalewajko K., Begelman M. C., Sikora M., 2014, ApJ, 789, 161
Nenkova M., Sirocky M. M., Nikutta R., Ivezić Ž., Elitzur M., 2008, ApJ, 685, 160
Nolan P. et al., 2012, ApJS, 199, 31
Orienti M. et al., 2013, MNRAS, 428, 2418
Osterbrock D. E., Pogge R. W., 1985, ApJ, 297, 166
Pacciani L., Tavecchio F., Donnarumma I., Stamerra A., Carrasco L., Recillas E., Porras A., Uemura M., 2014, ApJ, 790, 45
Perlman E. S., 2000, in Dingus B. L., Salamon M. H., Kieda D. B., eds, AIP Conf. Proc. Vol. 515, GeV-TeV Gamma Ray Astrophysic Workshop: Towards a Major Atmospheric Cherenkov Detector VI. Am. Inst. Phys., New York, p. 53
Pogge R. W., 2000, New Astron. Rev., 44, 381
Poutanen J., Stern B., 2010, ApJ, 717, L118
Raiteri C. M. et al., 2011, A&A, 534, 87
Raiteri C. M. et al., 2012, A&A, 545, 48
Richards J. L. et al., 2011, ApJS, 194, 29
Rolke W. A., López A. M., Conrad J., 2005, Nucl. Instrum. Methods Phys. Res. A, 551, 493
Roming P. W. A. et al., 2005, Space Sci. Rev., 120, 95
Saito S., Stawarz Ł., Tanaka Y. T., Takahashi T., Madejski G., D'Ammando F., 2013, ApJ, 766, L11
Schneider D. P. et al., 2010, AJ, 139, 2360
Sol H. et al., 2013, Astropart. Phys., 43, 215
Steiner J. F., Narayan R., McClintock J. E., Ebisawa K., 2009, PASP, 121, 1279
Stern B. E., Poutanen J., 2011, MNRAS, 417, L11
Stern B. E., Poutanen J., 2014, AJ, 794, 8
Tavecchio F., Ghisellini G., Bonnoli G., Ghirlanda G., 2010, MNRAS, 405, L94
Urry M., Padovani P., 1995, PASP, 107, 803
Wilms J., Allen A., McCray R., 2000, ApJ, 542, 914
Zhou H.-Y., Wang T.-G., Dong X.-B., Zhou Y.-Y., Li C., 2003, ApJ, 584, 147

[1]*Dipartimento di Fisica e Astronomia, Universitá degli Studi di Bologna, Viale Berti Pichat, 6/2. I-40127 Bologna, Italy*
[2]*INAF – Istituto di Radioastronomia, Via Gobetti 101, I-40129 Bologna, Italy*
[3]*U.S. Naval Research Laboratory, Code 7653, 4555 Overlook Ave SW, Washington, DC 20375-5352, USA*
[4]*INAF – Osservatorio Astrofisico di Torino, Via Osservatorio 20, I-10025 Pino Torinese (TO), Italy*
[5]*Cahill Center for Astronomy and Astrophysics, California Institute of Technology 1200 E. California Blvd, Pasadena, CA 91125, USA*
[6]*KTH, Department of Physics, and the Oskar Klein Centre, AlbaNova, SE-106 91 Stockholm, Sweden*
[7]*National Radio Astronomy Observatory (NRAO), PO Box 0, Socorro, NM 87801, USA*
[8]*NASA Goddard Space Flight Center, Greenbelt, MD 20771, USA*
[9]*Department of Physics, Purdue University, Northwestern Avenue 525, West Lafayette, IN 47907, USA*
[10]*Department of Physics, Washington University, St. Louis, MO 63130, USA*
[11]*Fred Lawrence Whipple Observatory, Harvard-Smithsonian Center for Astrophysics, Amado, AZ 85645, USA*
[12]*Department of Physics and Astronomy and the Bartol Research Institute, University of Delaware, Newark, DE 19716, USA*
[13]*School of Physics, University College Dublin, Belfield, Dublin 4, Ireland*
[14]*Department of Physics and Astronomy, Iowa State University, Ames, IA 50011, USA*
[15]*Institute of Physics and Astronomy, University of Potsdam, D-14476 Potsdam-Golm, Germany*
[16]*DESY, Platanenallee 6, D-15738 Zeuthen, Germany*
[17]*Astronomy Department, Adler Planetarium and Astronomy Museum, Chicago, IL 60605, USA*
[18]*Department of Physics and Astronomy, Barnard College, Columbia University, NY 10027, USA*
[19]*Department of Astronomy and Astrophysics, 525 Davey Lab, Pennsylvania State University, University Park, PA 16802, USA*
[20]*School of Physics and Astronomy, University of Minnesota, Minneapolis, MN 55455, USA*
[21]*Santa Cruz Institute for Particle Physics and Department of Physics, University of California, Santa Cruz, CA 95064, USA*
[22]*School of Physics, National University of Ireland Galway, University Road, Galway, Ireland*
[23]*Department of Physics and Astronomy, University of Iowa, Van Allen Hall, Iowa City, IA 52242, USA*
[24]*Physics Department, Columbia University, New York, NY 10027, USA*
[25]*Department of Physics and Astronomy, University of Utah, Salt Lake City, UT 84112, USA*
[26]*Department of Physics and Astronomy, DePauw University, Greencastle, IN 46135-0037, USA*
[27]*Kavli Institute for Cosmological Physics, University of Chicago, Chicago, IL 60637, USA*
[28]*School of Physics and Center for Relativistic Astrophysics, Georgia Institute of Technology, 837 State Street NW, Atlanta, GA 30332-0430, USA*
[29]*Department of Physics and Astronomy, University of California, Los Angeles, CA 90095, USA*
[30]*Physics Department, McGill University, Montreal, QC H3A 2T8, Canada*
[31]*Department of Applied Physics and Instrumentation, Cork Institute of Technology, Bishopstown, Cork, Ireland*
[32]*Enrico Fermi Institute, University of Chicago, Chicago, IL 60637, USA*
[33]*Argonne National Laboratory, 9700 S. Cass Avenue, Argonne, IL 60439, USA*

This paper has been typeset from a TEX/LATEX file prepared by the author.